

Electrochemical water oxidation by a copper complex with N₄-donor ligand at neutral condition

Junqi Lin*, Xin Chen, Nini Wang, Shanshan Liu, Zhijun Ruan*, Yanmei Chen*

Hubei Key Laboratory of Processing and Application of Catalytic Materials, College of Chemistry and Chemical Engineering, Huanggang Normal University, Huanggang, 438000 China

* To whom correspondence should be addressed.

E-mail addresses: linjunqi@hgnu.edu.cn, ruanzhijun@hgnu.edu.cn, cingym@163.com

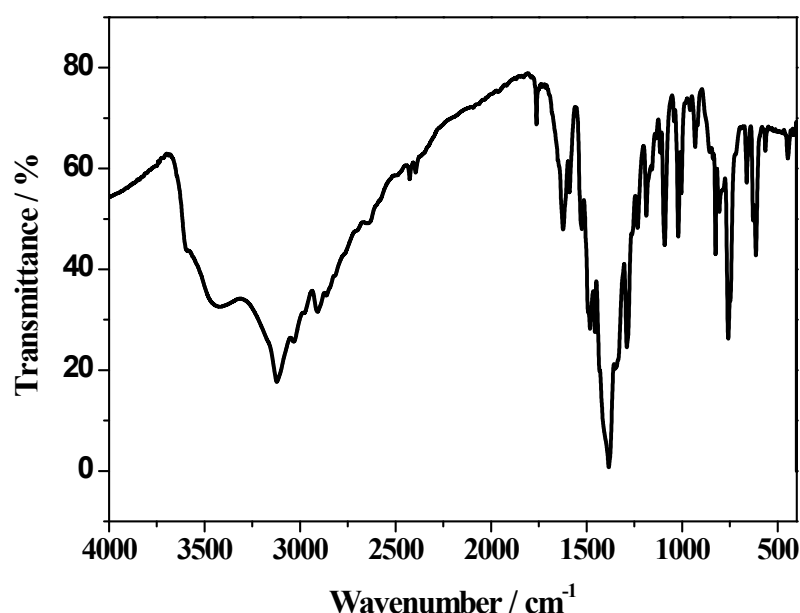


Figure S1. The FTIR spectrum of [Cu^{II}(H₂L)](NO₃)₂.

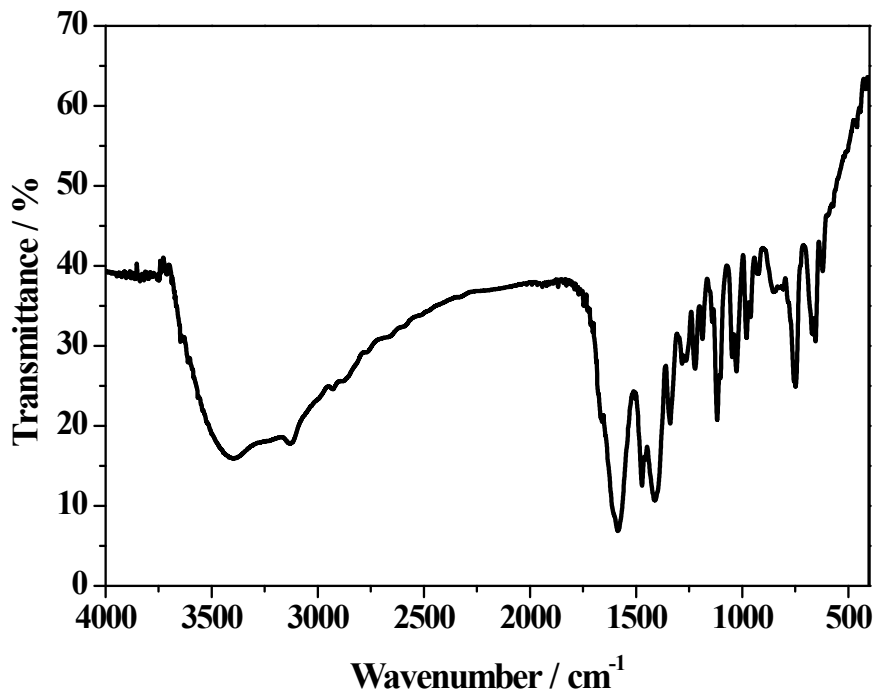


Figure S2. The IR spectrum of $[\text{Zn}^{\text{II}}(\text{H}_2\text{L})](\text{OAc})_2$.

Acquisition Parameter						
Polarity	Positive	n/a	n/a	No. of Laser Shots	100	
n/a	n/a	n/a	1	Laser Power	70.0 lp	
Broadband Low Mass	53.8 m/z	n/a	n/a	n/a	n/a	
Broadband High Mass	1000.0 m/z	n/a	n/a	n/a	n/a	
Acquisition Mode	Single MS	n/a	n/a	Calibration Date	Fri Feb 21 02:36:54 2014	
Pulse Program	basic	n/a	n/a	Data Acquisition Size	1048576	
Source Accumulation	0.100 sec	n/a	n/a	Apodization	Sine-Bell Multiplication	
Ion Accumulation Time	0.500 sec	n/a	n/a			
Flight Time to Acq. Cell	0.001 sec	n/a	n/a			

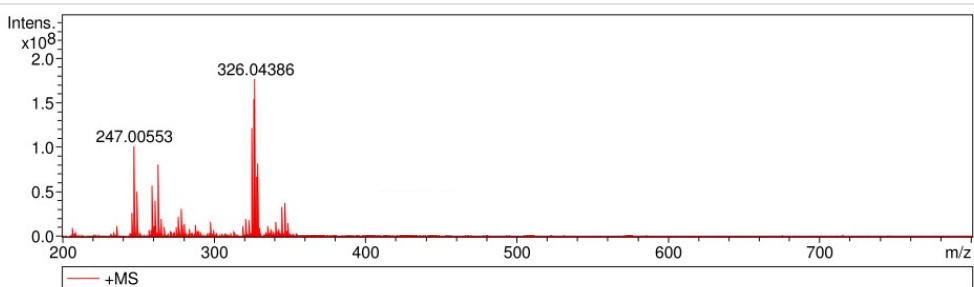


Figure S3. High resolution mass spectrum of **1** in water.

Acquisition Parameter					
Polarity	Positive	n/a	n/a	No. of Laser Shots	100
n/a	n/a	n/a	1	Laser Power	70.0 lp
Broadband Low Mass	53.8 m/z	n/a	n/a	n/a	n/a
Broadband High Mass	1000.0 m/z	n/a	n/a	n/a	n/a
Acquisition Mode	Single MS	n/a	n/a	Calibration Date	Fri Feb 21 02:36:54 2014
Pulse Program	basic	n/a	n/a	Data Acquisition Size	1048576
Source Accumulation	0.100 sec	n/a	n/a	Apodization	Sine-Bell Multiplication
Ion Accumulation Time	0.500 sec	n/a	n/a		
Flight Time to Acq. Cell	0.001 sec	n/a	n/a		

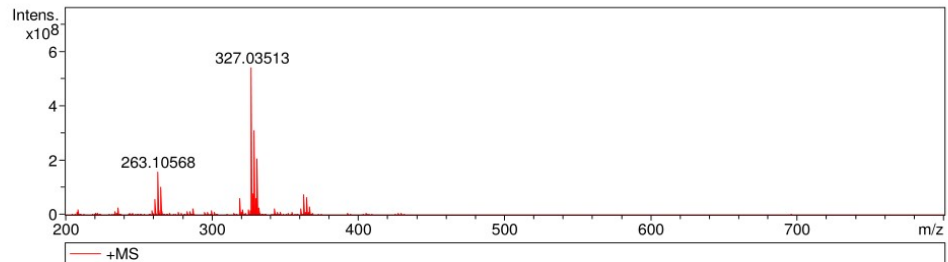


Figure S4. High resolution mass spectrum of **2** in water.

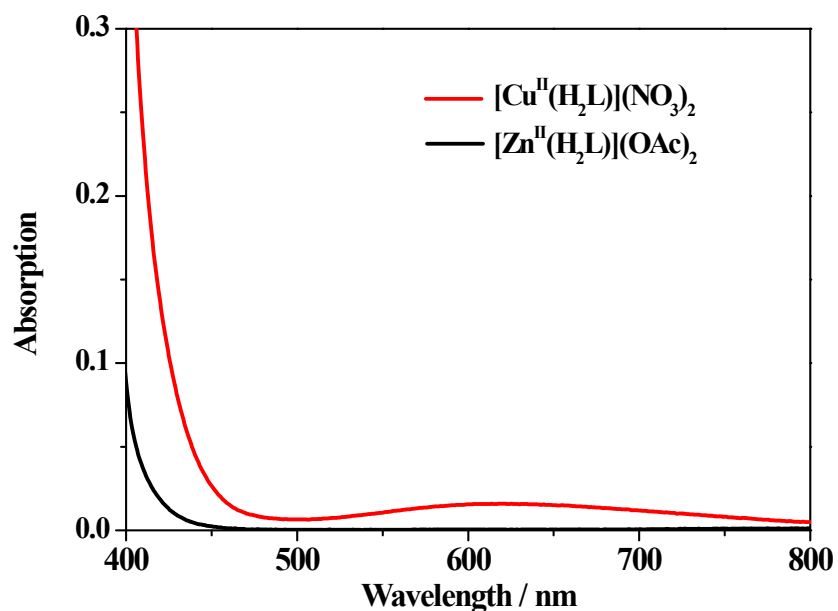


Figure S5. The UV-vis absorption spectrum of 0.1 mM of $[\text{Cu}^{\text{II}}(\text{H}_2\text{L})](\text{NO}_3)_2$ and 0.1 mM of $[\text{Zn}^{\text{II}}(\text{H}_2\text{L})](\text{OAc})_2$ in 0.1 M PBS at neutral condition.

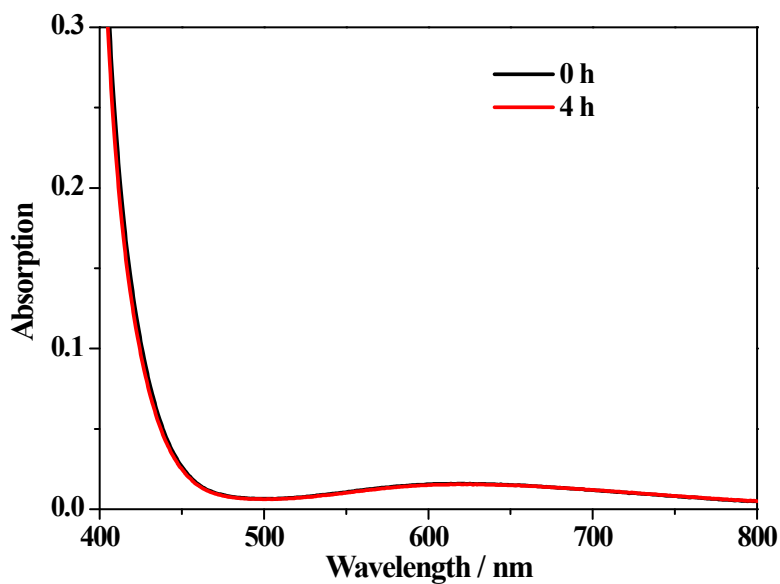


Figure S6. The UV-vis absorption spectrum of 0.1 mM of $[\text{Cu}^{\text{II}}(\text{H}_2\text{L})](\text{NO}_3)_2$ after aging for 4h in 0.1 M PBS at neutral condition.

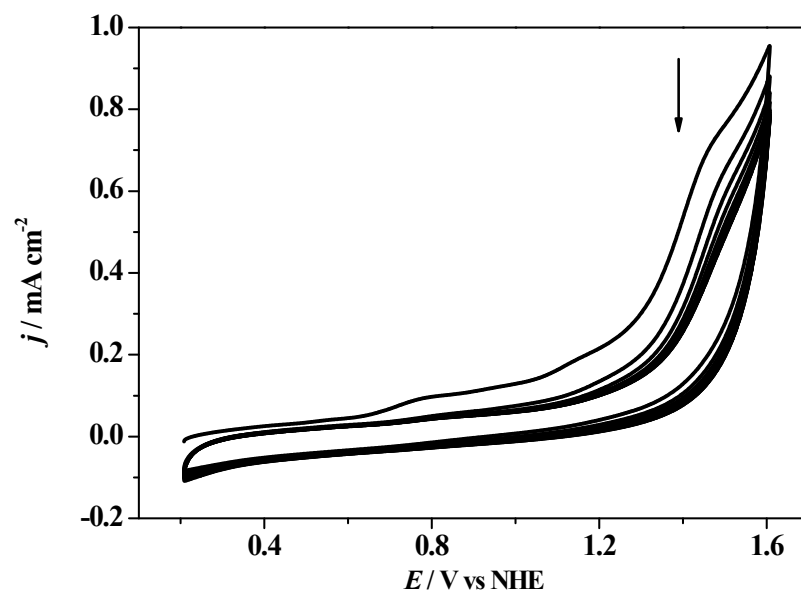


Figure S7. 10 times continuous CV scans of 0.1 mM of **1** in phosphate buffer solution at neutral condition, GC electrode as working electrode, scan rate = 100 mV/s.

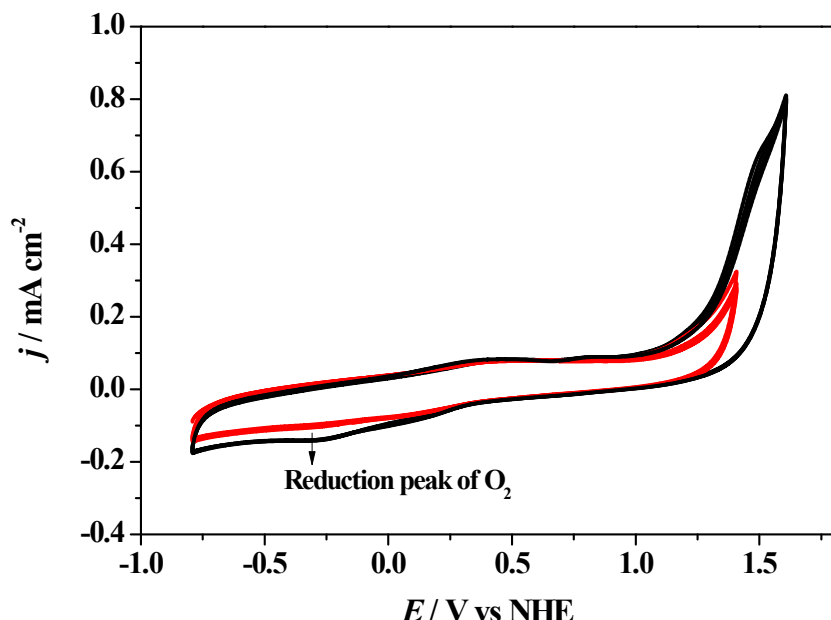


Figure S8. Control CV experiment that indicating the oxygen generation at the catalytic current. 0.1 mM of **1** in 0.1 M phosphate buffer solution at pH 7.0, scan rate = 100 mV/s.

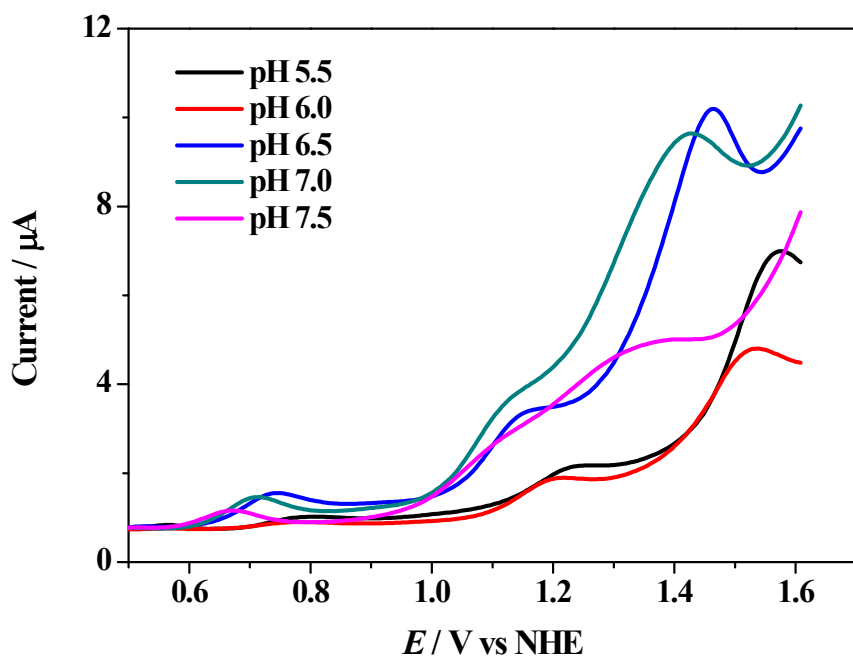


Figure S9. DPVs of 0.1 mM of **1** in 0.1 M phosphate buffer solution at different pH values. DPVs were obtained with the following parameters: amplitude. = 50 mV, step height = 4 mV, pulse width = 0.05 s, pulse period = 0.5 s and sampling width = 0.0167 s.

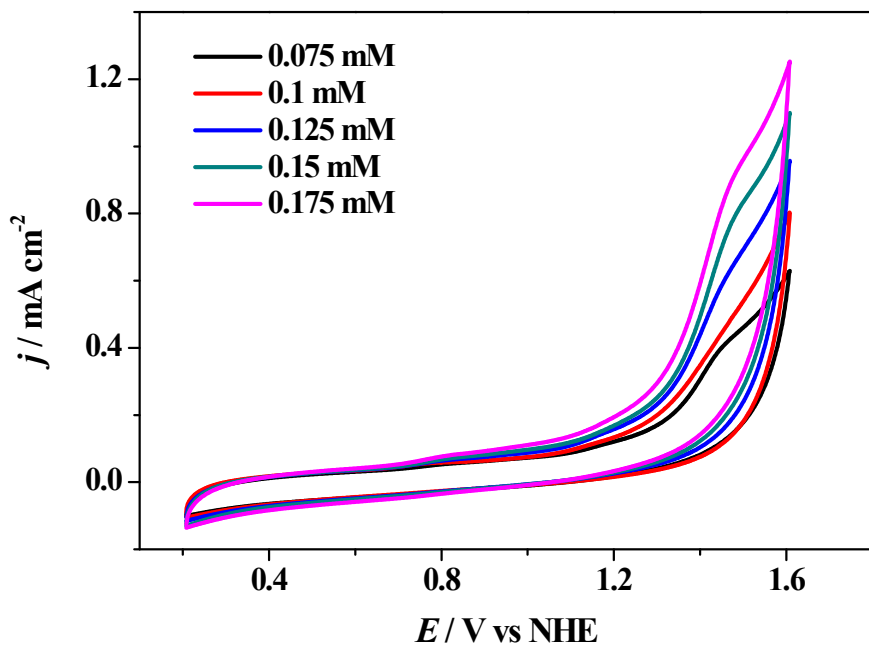


Figure S10. CVs of various concentration of **1** in 0.1 M phosphate buffer solution. Scan rate = 100 mV/s.

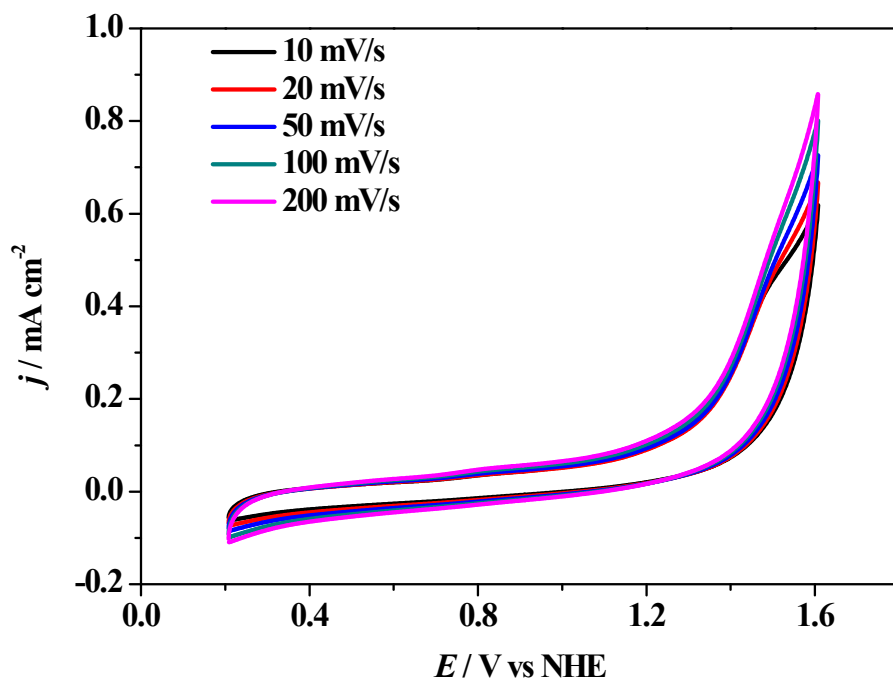


Figure S11. CVs of 0.1 mM of **1** in 0.1 M phosphate buffer solution at neutral condition with various scan rate.

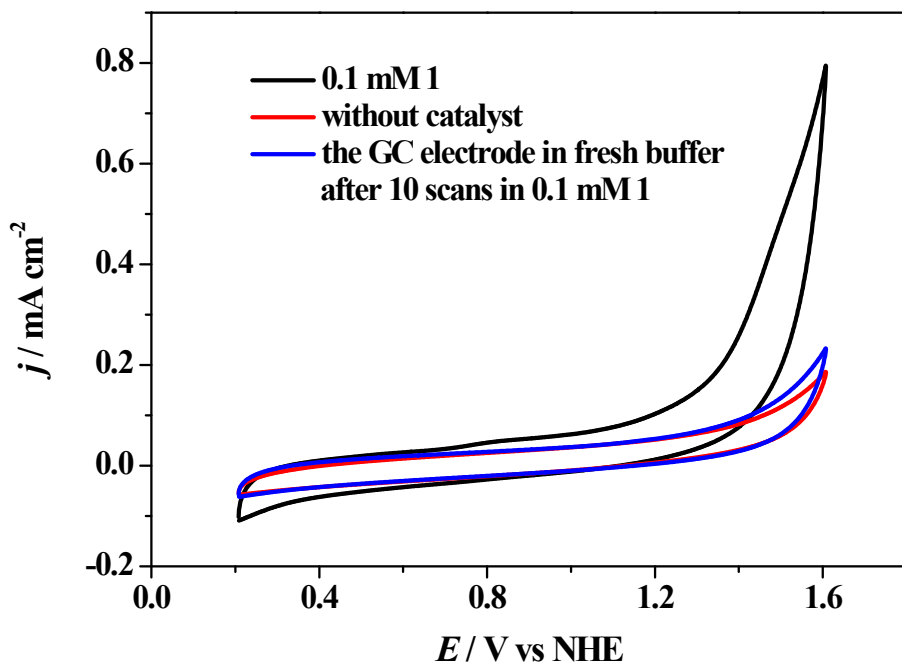


Figure S12. After multiple CV scans of 0.1 mM of **1** (black scan), the used GC electrode was rinsed by water but without polished, this electrode didn't show significant catalytic current in the same buffer solution (blue curve).

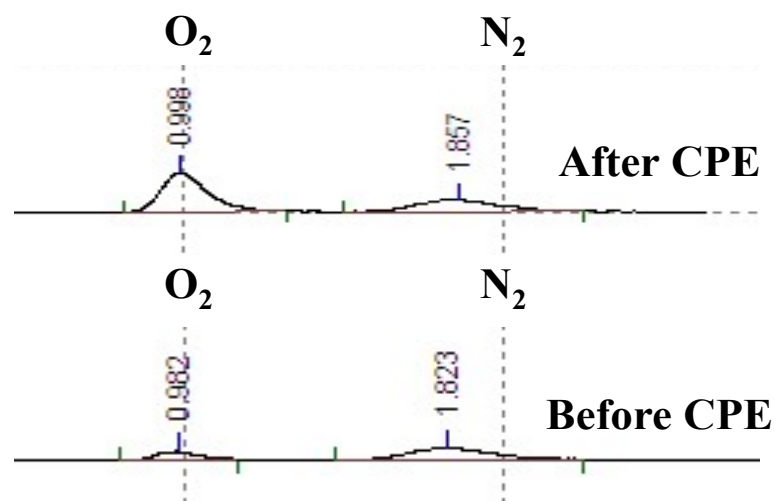


Figure S13. The gas chromatographic trace before and after CPE experiments.

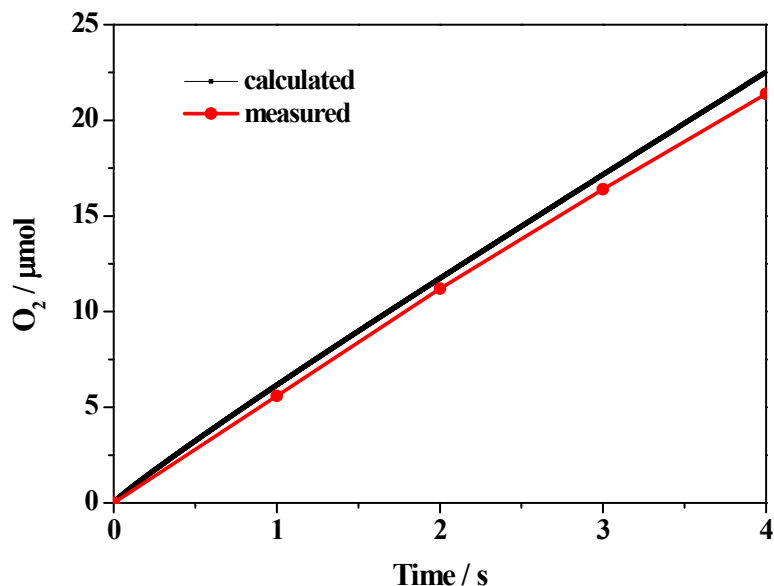


Figure S14. Faradaic efficiency of O_2 evolution for **1** in 0.1 M PBS at pH 7.0 at 1.6 V vs NHE for 4 h of electrolysis. The red line represents the amount of evolved O_2 quantified by GC analysis. The black line represents the amount of O_2 expected for a 100% Faraday efficiency according to the total passed charged during 4 h of electrolysis.

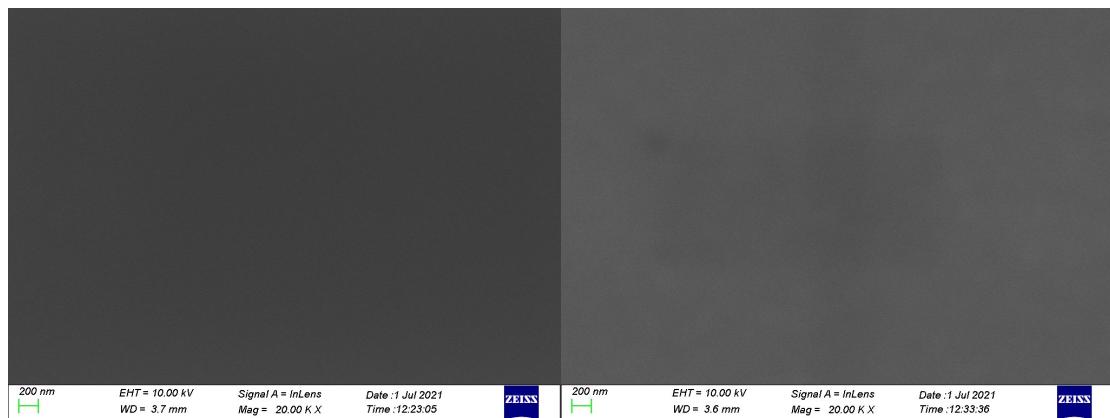


Figure S15. SEM images of the surface of ITO electrode before (left) and after (right) 4 h CPE experiments of **1** in 0.1 M phosphate buffer solution at neutral.

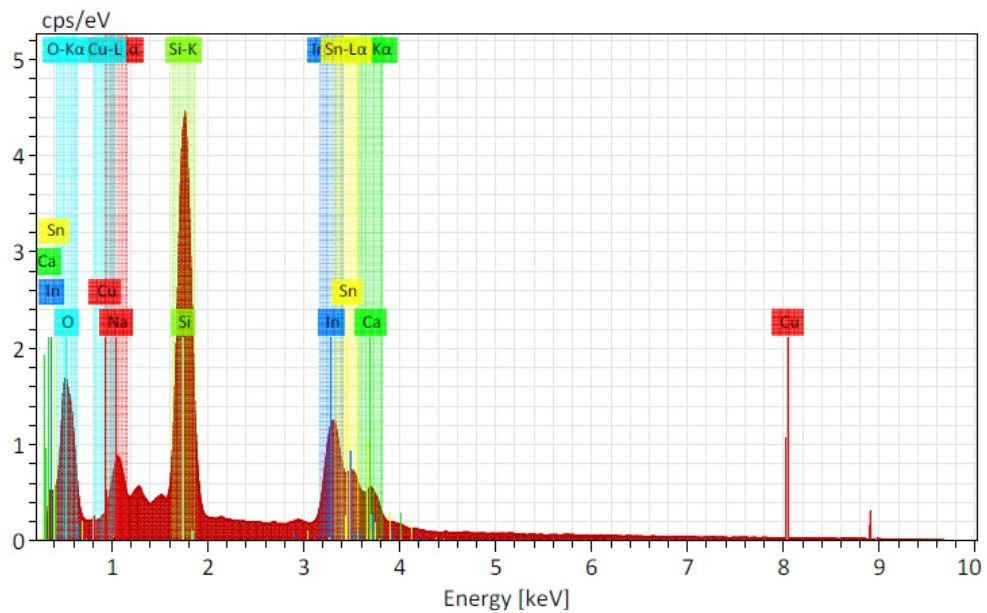


Figure S16. The EDX analysis of the ITO electrodes before CPE test.

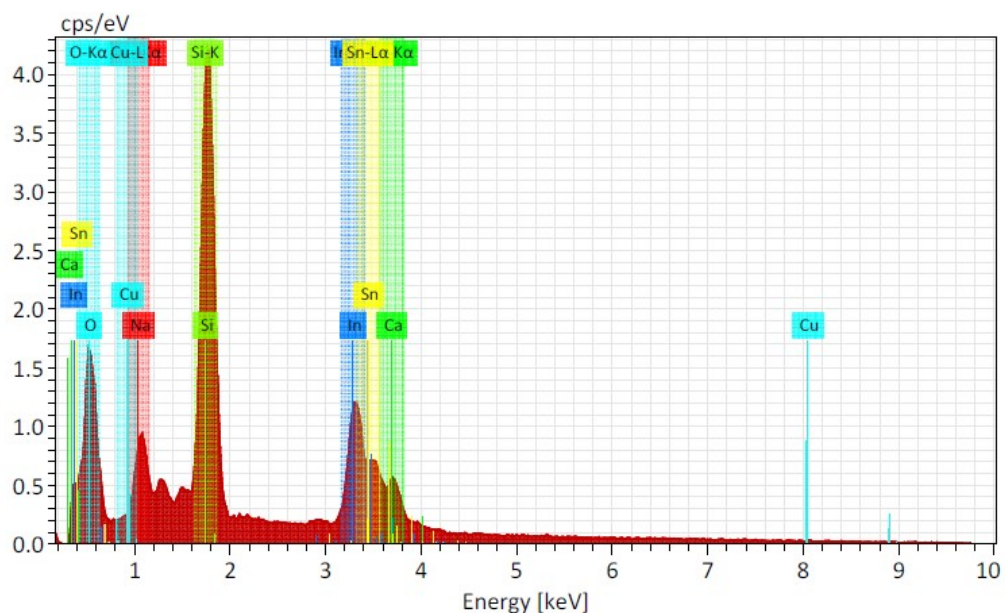


Figure S17. The EDX spectrum of the ITO electrodes after 4 h CPE test of **1**.

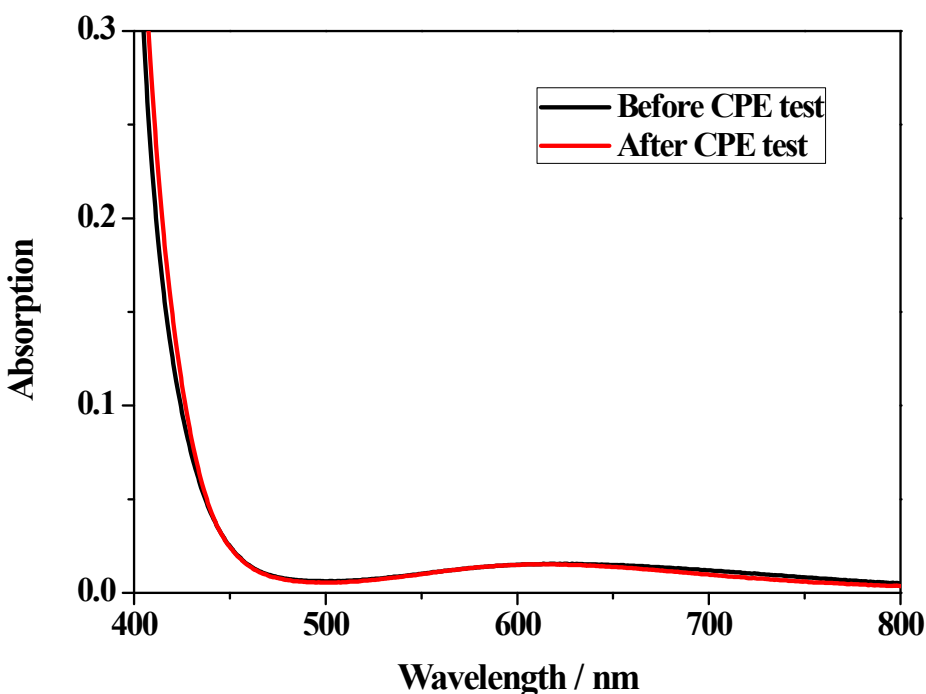


Figure S18. UV-vis absorption spectra of 0.1 mM of **1** before and after 4 h CPE test.

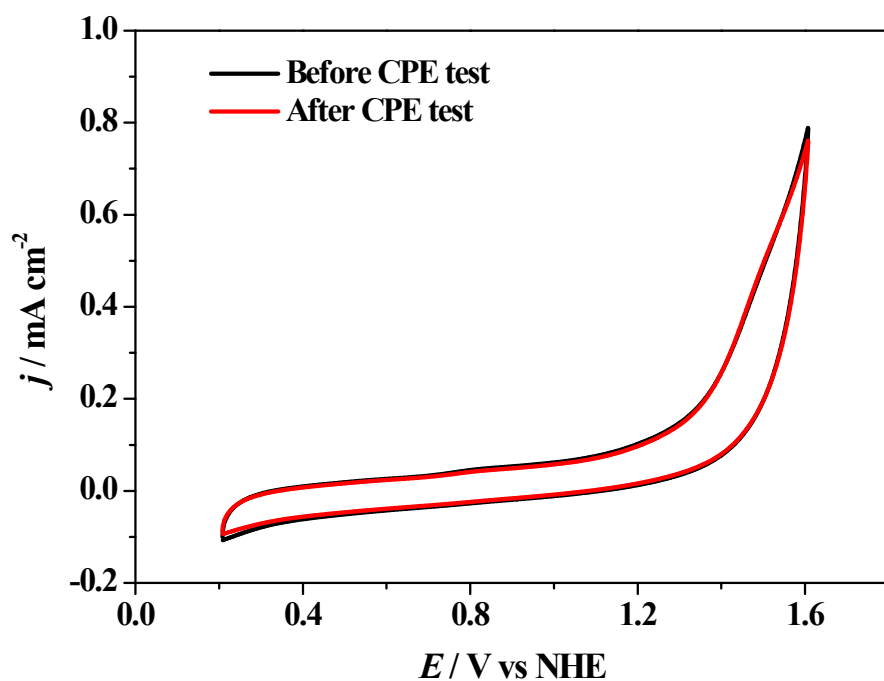
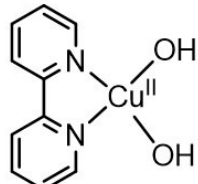


Figure S19. The CV curves of 0.1 mM complex **1** before and after 4 h CPE tests at 1.60 V vs NHE. 0.1 M PBS at pH 7.0 is used as electrolyte and scan rate = 100 mV/s.

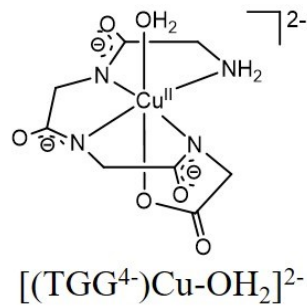
Table S1. Kinetic data of **1** and some reported Cu based homogeneous water oxidation electrocatalyst

Catalyst ^a	$k_{\text{cat}}/\text{s}^{-1}$	pH	Potential/V ^b	$\eta/\text{mV}^{\text{c}}$	Ref.
(bpy)Cu(OH) ₂	100	13.1	1.45	750	S1
[(TGG ⁴⁻)Cu-OH ₂] ²⁻	33	11.0	1.32	520	S2
[Cu(TMC)(H ₂ O)] ²⁺	30	7.0	1.63	580	S3
[Cu ₂ (BPMAN)(μ-OH)] ³⁺	0.6	7.0	1.62	800	S4
Cu ^{II} (Py3P)	20	8.0	1.50	440	S5
[L _{Glu} -Cu] ₄	105	12.0	1.56	880	S6
[L _{Gly} -Cu] ₄	267	12.0	1.70	880	S6
[Cu(Me ₂ oxpn)Cu(OH) ₂]	2.14	10.4	1.20	636	S7
[(opba)Cu] ²⁻	1.13	10.8	1.40	636	S8
CuMe ₄ cyclam	7	7.0	1.70	880	S9
[(Me ₂ TMPA)(μ-OH)Cu] ₂ ²⁻	33	12.5	1.82	636	S10
[Cu(pyalk) ₂]	0.7	12.5	1.13	550	S11
[L-Cu-CO ₃ H] ⁻	20.1	10.0	1.60	650	S12
[Cu ^{II} (L)] ²⁺	0.12	12	1.35	830	S13
[Cu(I)(C2)] ⁺	9.77	6.5	1.73	674	S14
[(L4)Cu] ²⁻	10.5	11.6	1.39	754	S15
[Cu(H ₂ L)] ²⁺	11.09	7.0	1.60	580	This work

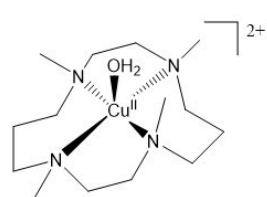
^a The structures of the catalysts listed in this table are given below. ^b Potential used for the calculation of k_{cat} (vs. NHE). ^c η = onset overpotential obtained from CV test.



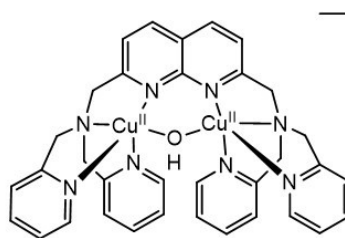
$(bpy)Cu(OH)_2$



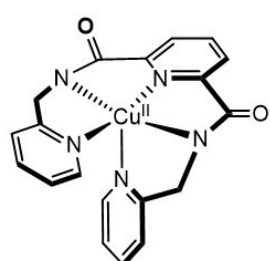
$[(TGG^{4-})Cu-OH_2]^{2-}$



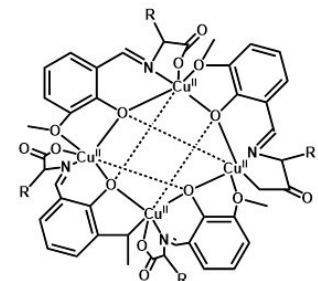
$[Cu(TMC)(H_2O)]^{2+}$



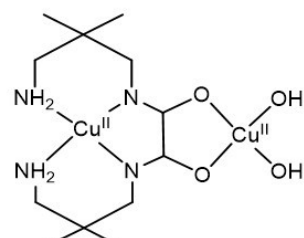
$[Cu_2(BPMAN)(\mu-OH)]^{3+}$



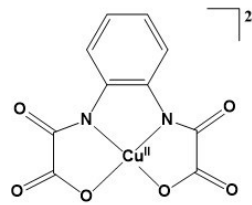
$Cu^{II}(Py_3P)$



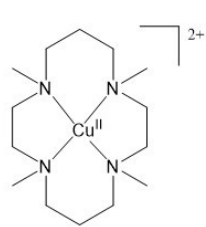
$R = CH_3 [L_{Glu}-Cu_4]$
 $R = H [L_{Gly}-Cu_4]$



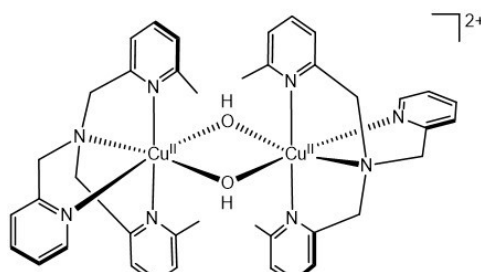
$[Cu(Me_2oxpn)Cu(OH)_2]$



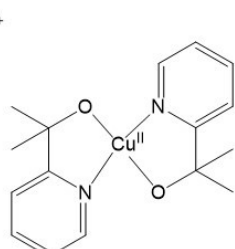
$[(opba)Cu]^{2-}$



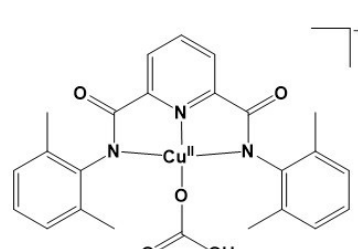
$CuMe_4cyclam$



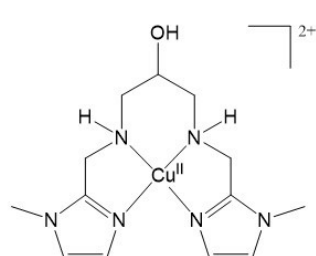
$[(Me_2TMPA)(\mu-OH)Cu]^{2+}$



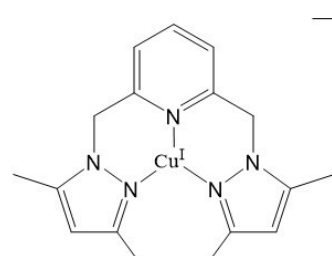
$[Cu(pyalk)_2]$



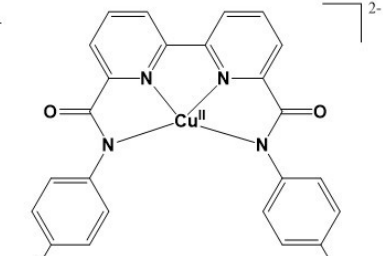
$[L-Cu-CO_3H]^-$



$[Cu^{II}(L)]^{2+}$



$[Cu^I(C_2)]^+$



$[L_4Cu]^{2-}$

Reference

- S1 S. M. Barnett, K. I. Goldberg and J. M. Mayer, *Nat. Chem.*, 2012, **4**, 498–502.
- S2 M.-T. Zhang, Z. Chen, P. Kang and T. J. Meyer, *J. Am. Chem. Soc.*, 2013, **135**, 2048–2051.
- S3 F. Yu, F. Li, J. Hu, L. Bai, Y. Zhu and L. Sun, *Chem. Commun.*, 2016, **52**, 10377–10380.
- S4 X.-J. Su, M. Gao, L. Jiao, R.-Z. Liao, P. E. M. Siegbahn, J.-P. Cheng and M.-T. Zhang, *Angew. Chem. Int. Ed.*, 2015, **54**, 4909–4914.
- S5 M. K. Coggins, M. T. Zhang, N. Song and T. J. Meyer, *Angew. Chem. Int. Ed.*, 2014, **53**, 12226–12230.
- S6 X. Jiang, J. Li, B. Yang, X-Z. Wei, B-W. Dong, Y. Kao, M-Y. Huang, C-H Tung, and Li-Zhu Wu, *Angew. Chem. Int. Ed.*, 2018, **57**, 7850–7854.
- S7 L.-L. Zhou, T. Fang, J.-P. Cao, Z.-H. Zhu, X.-T. Su and S.-Z. Zhan, *J. Power Sources.*, 2015, **273**, 298–304.
- S8 L.-Z. Fu, T. Fang, L.-L. Zhou and S.-Z. Zhan, *RSC Adv.*, 2014, **4**, 53674–53680.
- S9 A. Prevedello, I. Bazzan, N. D. Carbonare, A. Giuliani, S. Bhardwaj, C. Africh, C. Cepek, R. Argazzi, M. Bonchio, S. Caramori, M. Robert and A. Sartorel, *Chem. Asian J.*, 2016, **11**, 1281–1287.
- S10 S. J. Koepke, K. M. Light, P. E. VanNatta, K. M. Wiley and M. T. Kieber-Emmons, *J. Am. Chem. Soc.*, 2017, **139**, 8586–8600.
- S11 K. J. Fisher, K. L. Materna, B. Q. Mercado, R. H. Crabtree and G. W. Brudvig, *ACS Catal.*, 2017, **7**, 3384–3387.
- S12 F. Chen, N. Wang. H. Lei, D. Guo, H. Liu, Z. Zhang, W. Zhang, W. Lai and R. Cao, *Inorg. Chem.*, 2017, **56**, 13368–13375
- S13 S. Nestke, E. Ronge and I. Siewert. *Dalton Trans.*, 2018, **47**, 10737-10741.
- S14 T. Makhado, B. Das, R. J. Kriek, H. C. M. Vosloo and A. J. Swarts, *Sustainable Energy Fuels.*, 2021, **5**, 2771-2780.
- S15 M. Gil-Sepulcre, P. Garrido-Barros, J. Oldengott, I. Funes-Ardoiz, R. Bofill, X. Sala, J. Benet-Buchholz and A. Llobet, *Angew. Chem. Int. Ed.*, DOI: 10.1002/anie.202104020.